Quantification of the Effect of 4-*tert*-Butylpyridine Addition to I^-/I_3^- Redox Electrolytes in Dye-Sensitized Nanostructured TiO_2 Solar Cells

Gerrit Boschloo,* Leif Häggman, and Anders Hagfeldt

Center of Molecular Devices, Department of Chemistry, Royal Institute of Technology, Teknikringen 30, SE-10044 Stockholm, Sweden

Received: March 30, 2006; In Final Form: May 15, 2006

Addition of 4-*tert*-butylpyridine (4TBP) to redox electrolytes used in dye-sensitized TiO_2 solar cells has a large effect on their performance. In an electrolyte containing 0.7 M LiI and 0.05 M I_2 in 3-methoxypropionitrile, addition of 0.5 M 4TBP gave an increase of the open-circuit potential of 260 mV. Using charge extraction and electron lifetime measurements, this increases could be attributed to a shift of the TiO_2 band edge toward negative potentials (responsible for 60% of the voltage increase) and to an increase of the electron lifetime (40%). At a lower 4TBP concentration the shift of the band edge was similar, but the effect on the electron lifetime was less pronounced. The working mechanism of 4TBP can be summarized as follows: (1) 4TBP affects the surface charge of TiO_2 by decreasing the amount of adsorbed protons and/or Li^+ ions. (2) It decreases the recombination of electrons in TiO_2 with triiodide in the electrolyte by preventing triiodide access to the TiO_2 surface and/or by complexation with iodine in the electrolyte.

Introduction

Dye-sensitized solar cells (DSCs) based on mesoporous TiO_2 films and ruthenium sensitizers have received much attention in recent years.[1−3] DSCs are photoelectrochemical solar cells that contain a (usually liquid) electrolyte. A redox couple in this electrolyte is used to regenerate the oxidized dye molecules and to carry positive charge to the counter electrode. The triiodide/iodide (I_3^-/I^-) redox couple is by far the most frequently used in DSCs, although several alternatives have been developed, such as cobalt complexes[4,5] and pseudohalogens.[6,7] The performance of the triiodide/iodide system is, however, still unmatched.

The precise composition of the triiodide/iodide electrolyte affects the performance of the dye-sensitized solar cell significantly. The type of cation of the iodide salt is important for the resulting photovoltage and the photocurrent.[8,9] Ultrafast laser spectroscopy studies have shown that the kinetics of electron injection are affected by the choice of cation.[10,11] Furthermore, regeneration of oxidized dye molecules is also influenced by the type of cation.[12] A general explanation is that different cations adsorb at the TiO_2 surface to different extents, thereby affecting the surface charge and the band edge position of the conduction band (and other energetic states in the metal oxide). Adsorbed positive charge has in turn an effect on the local concentration of iodide ions.

Significant improvement of the solar cell performance can be obtained by the addition of certain compounds to the electrolyte. The most frequently used additive is 4-*tert*-butylpyridine (4TBP).[2,9,13−16] 4TBP gives a significant improvement of the open-circuit potential, V_{OC}, of the solar cell, while the short-circuit current is not much affected or slightly decreased. Several mechanisms have been proposed to explain the observed effects. Nazeeruddin et al. showed that the dark current, due to reduction of triiodide by electrons in TiO_2, was suppressed by addition of 4TBP.[2] This was attributed to a blocking effect due to adsorption of 4TBP on active sites at the TiO_2 surface. Huang et al. estimated that addition of 4TBP and similar compounds decreased the electron−triiodide recombination rate by 1−2 orders of magnitude.[13] Schlichthörl et al. found that 4TBP addition led to a shift of the TiO_2 conduction band edge as well as an increased electron lifetime.[14] Nakade and co-workers, on the other hand, found no significant influence of 4TBP on the electron lifetime and attributed the increased V_{OC} solely to a shift of the band edge.[9] Boschloo et al. found that addition of 4TBP led to a decreased response in the red part of the photocurrent spectrum, which is in accordance with a band edge shift of TiO_2.[15]

Most studies using dye-sensitized solar cells suggest that 4TBP is active at the TiO_2−electrolyte interface. Infrared spectroscopy, Raman spectroscopy, and XPS give evidence that 4TBP binds at the TiO_2 surface.[17] An alternative explanation, however, may be that 4TBP affects the electrolyte. Pyridine is known to form stable molecular complexes with iodine.[18,19] 4TBP could form similar complexes with iodine, which could play an important role in the DSC.[20,21]

In this study we will focus on the precise action of 4TBP in the dye-sensitized solar cell by combining a number of experimental techniques. The results suggest that the action of 4TBP is both at the semiconductor−electrolyte interface, where it affects the surface charge, and in the electrolyte, where it forms a complex with iodine.

Experimental Section

Mesoporous TiO_2 electrodes were prepared on conducting glass substrates (TEC 8, Pilkington) by compression of TiO_2 powder (Degussa P25) at 1360 kg cm^{-2}, followed by heating to 450 °C for 0.5 h.[22] The electrodes were immersed in a 0.5 mM ethanolic solution of N719 dye ($(TBA)_2$-*cis*-$Ru(Hdcbpy)_2(NCS)_2$, Solaronix, Switzerland) while still hot (80 °C) and left overnight. After being rinsed with ethanol and drying, the

* To whom correspondence should be addressed. E-mail: gerrit@kth.se.

10.1021/jp0619641 CCC: $33.50
Published on Web 06/15/2006

electrodes were assembled with a counter electrode (thermally platinized TEC 8) using a thermoplastic frame. Redox electrolyte was introduced through small holes drilled in the counter electrode that were sealed afterward. The composition of the electrolyte was as follows: 0.05 M I_2 and 0.7 M LiI in 3-methoxypropionitrile (3MPN), with 0, 55, or 500 mM 4-*tert*-butylpyridine. Nine solar cells were prepared, three with each electrolyte composition, all having a TiO_2 film thickness of 13 μm. Cells with identical electrolytes gave highly reproducible results. The power conversion efficiency of the solar cells ranged from 3.7% to 5.1%, depending on the 4TBP concentration. The active area of the cells was 0.785 cm^2.

Electron concentrations, lifetimes, and transport times in the dye-sensitized TiO_2 solar cells were measured in a system using a red-light-emitting diode (Luxeon Star 1W, $\lambda_{max} = 640$ nm) as the light source. Voltage or current traces were recorded using a 16-bit resolution data acquisition board (DAQ National Instruments) in combination with a current amplifier (Stanford Research Systems SR570) and a custom-made system using electromagnetic relay switches. The relation between potential and charge was investigated using a combined voltage decay/charge extraction method, similar to that developed by Duffy et al.[23,24] The solar cell was illuminated for 5 s under open-circuit conditions, and the voltage was left to decay for a certain period in the dark to a voltage V. Then the cell was short-circuited, and the current was measured and integrated over 10 s to obtain $Q_{OC}(V)$. The charge accumulated in the TiO_2 film under short-circuit conditions, Q_{SC}, was determined using photocurrent transients. The light source was switched off, and the photocurrent transient was integrated over 10 s to obtain Q_{SC}. The internal potential in the TiO_2 film under short-circuit conditions was estimated using another switching experiment. The solar cell was illuminated for 5 s under short-circuit conditions before, simultaneously, the light was switched off and the cell switched to open circuit. The voltage that develops, referred to as V_{SC}, gives a good indication of the electrochemical potential under short-circuit conditions.[24] Electron lifetimes and transport times were determined by monitoring the transient photovoltage and photocurrent response after a small change in light intensity. To the base light intensity was added a small square wave modulation (<10% intensity, 0.5 Hz), and the step response was recorded using the DAQ board. The current and voltage responses were well fitted using first-order decay kinetics, and time constants were obtained accordingly. The direction of illumination was always from the TiO_2 electrode side. All reported measurements were recorded about one week after cell preparation. Special care was taken not to expose the solar cells to high light intensities for long times, to prevent significant intercalation of Li^+ ions, which affects the measured time constants and extracted charge significantly.[25]

Electrochemical experiments were performed using a CH Instruments 660A potentiostat. The redox potential of the electrolytes was determined from the potential difference between a Pt wire, immersed in the redox electrolyte, and a Ag/Ag^+ reference electrode in a compartment containing 0.5 M lithium triflate in 3-methoxypropionitrile, separated from the redox electrolyte by a porous plug. Cyclic voltammetry was performed in a standard three-electrode cell with a 2 mm diameter Pt working electrode. The reference electrode was calibrated against the ferrocene/ferrocenium redox couple.

Results

Addition of 4-*tert*-butylpyridine to the redox electrolyte gives a significant improvement of the dye-sensitized TiO_2 solar cell performance, as is well-documented in the literature.[2,9,13,15,16] The main effect of 4TBP is the improvement of the open-circuit potential (V_{OC}); see Figure 1a. Addition of 500 mM 4TBP increased V_{OC} by 260 mV. There is a logarithmical increase of V_{OC} with light intensity, with slopes of 70, 91, and 90 mV per decade for electrolytes with 0, 55, and 500 mM 4TBP, respectively. The short-circuit current density was not affected by addition of 55 mM 4TBP, but decreased by ~20% when 500 mM was added (data not shown). The decrease in photocurrent can be ascribed to a decreased electron injection efficiency,[15] as results presented below clearly indicate that charge collection of injected electrons will be improved upon addition of 4TBP.

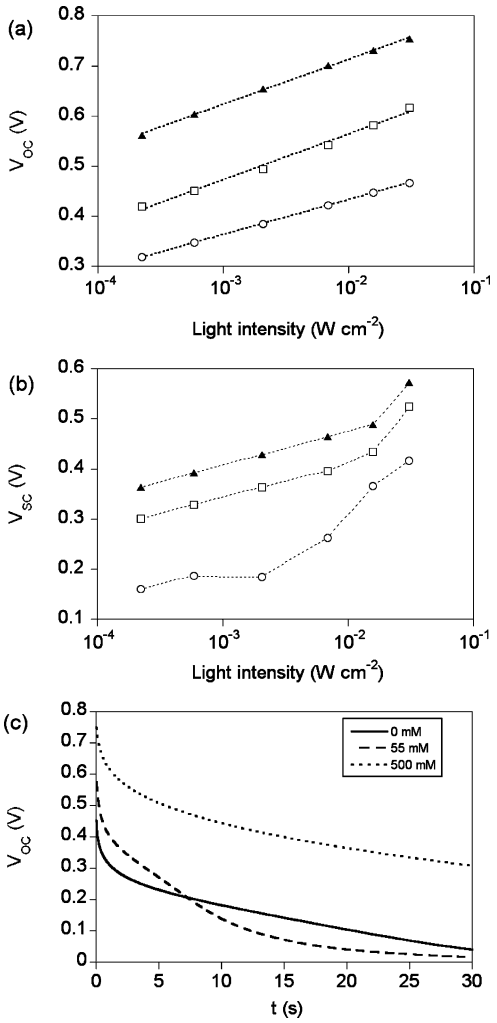

Figure 1. Light intensity dependence of the potential of dye-sensitized TiO_2 solar cells with different concentrations of 4TBP in the electrolyte: 0 mM (circles), 55 mM (squares), 500 mM (triangles); (a) open-circuit potential, V_{OC}, (b) internal potential in the TiO_2 film under short-circuit conditions, V_{SC}, (c) decay transients of the open-circuit potential. Illumination was with monochromatic light, $\lambda = 640$ nm. The light was switched off at $t = 0$ s.

The internal potential of the TiO_2 film in the illuminated solar cell operating under short-circuit conditions was estimated using a switching technique that is described in detail elsewhere.[24] Results are shown in Figure 1b. The trends observed in the internal potential V_{SC} are similar to those of V_{OC}: V_{SC} increases approximately logarithmically with light intensity, and addition of 4TBP leads to a higher V_{SC}. The somewhat deviating behavior of V_{SC} in the case of 0 mM 4TBP may be ascribed to the relatively short electron lifetimes found for these cells, which will be shown later. Short lifetimes will result in an underes-

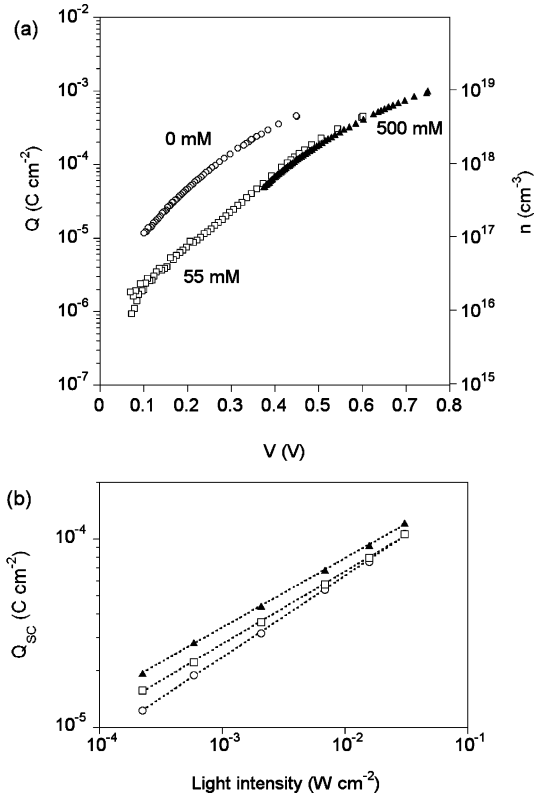

Figure 2. (a) Extracted charge and electron density as a function of the open-circuit potential in dye-sensitized TiO_2 solar cells. The 4TBP concentration in the electrolyte is indicated. (b) Extracted charge under short-circuit conditions as a function of the light intensity. 4TBP concentration: 0 mM (circles), 55 mM (squares), 500 mM (triangles).

timation of V_{SC}, as part of the electrons recombine before the maximum voltage is attained. It is interesting to note the difference between V_{OC} and V_{SC}: it is on average 0.13, 0.13, and 0.22 V for 0, 55, and 500 mM 4TBP, respectively.

Open-circuit potential decay transients of the dye-sensitized nanostructured TiO_2 solar cells are shown in Figure 1c. The light source is switched off at $t = 0$ s. While the voltage of solar cells with 0 or 55 mM 4TBP has decreased to less than 50 mV after 30 s, it is still more than 300 mV for cells with 500 mM 4TBP. It is further noted that the traces for cells with 0 and 500 mM are approximately parallel, whereas the 55 mM cell shows a different decay behavior.

The relation between charge and open-circuit potential in dye-sensitized nanostructured TiO_2 solar cells with the different electrolytes is shown in Figure 2a. A significant shift occurs upon addition of 4TBP to the redox electrolyte: the amount of extracted charge at a given voltage is lowered by a factor of ~5 after addition of the additive. No significant difference is found between 55 and 500 mM 4TBP. The electron density in TiO_2, shown on the right *y* axis, was calculated from the extracted charge using the thickness and the porosity of the TiO_2 film (~52%). No correction was made for charge accumulated at the conducting glass substrate−electrolyte interface. The highest electron density, 10^{19} cm^{-3}, corresponds to about 80 electrons per TiO_2 particle, assuming spherical 25 nm sized particles.

The charge present in the mesoporous TiO_2 film under short-circuit conditions was also determined by charge extraction; see Figure 2b. There is a power-law relation between Q_{SC} and light intensity, as noticed before.[24−26] Slightly more charge is extracted from solar cells with 4TBP in the electrolyte. The

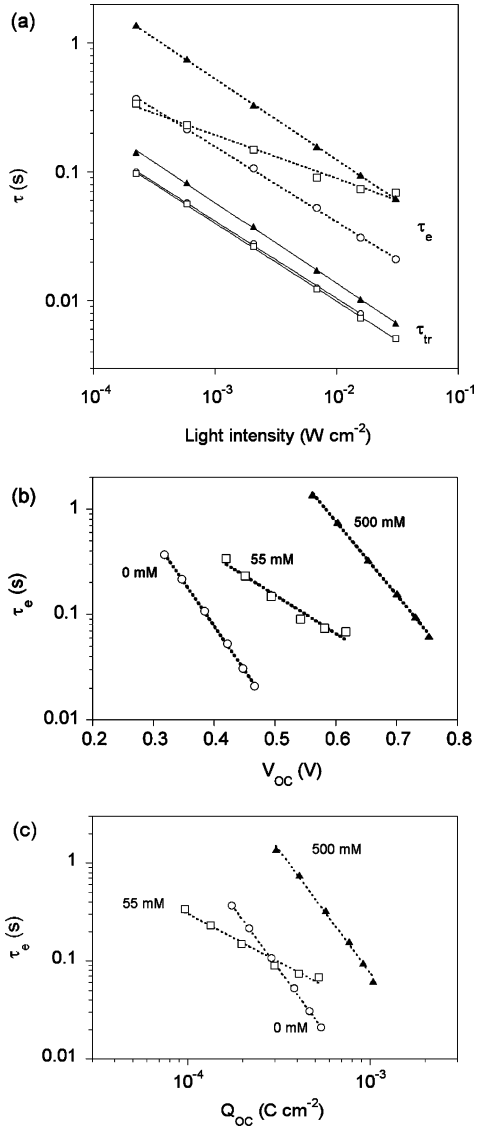

Figure 3. (a) Electron transport times τ_{tr} and lifetimes τ_e as functions of the light intensity. Time constants were determined using time-resolved small light modulation techniques. The dotted lines correspond to power-law fits. 4TBP concentration: 0 mM (circles), 55 mM (squares), 500 mM (triangles). (b) τ_e as a function of the open-circuit potential. The dotted lines correspond to exponential fits. (c) τ_e as a function of the extracted charge. The dotted lines correspond to power-law fits.

slopes in the log−log plot were similar for the investigated solar cells, ca. 0.4.

Electron transport times and electron lifetimes were measured using time-resolved techniques. A small square wave modulation was superimposed on the base light intensity, and the photocurrent or photovoltage was monitored. These time-resolved measurements were found to give essentially the same results as the comparable frequency-resolved techniques intensity-modulated photocurrent and photovoltage spectroscopy (IMPS and IMVS, respectively), but they are less time-consuming. Time-resolved small modulation techniques have been used previously for measurements of electron transport[27] and lifetime[9,28] in dye-sensitized solar cells. The effect of 4TBP addition to the electrolyte on electron transport times and lifetimes is shown in Figure 3a. The electron transport under short-circuit conditions is only slightly affected by the 4TBP concentration. A small increase of the transport time can be observed at the higher concentration. The exponent of the power-law fits of

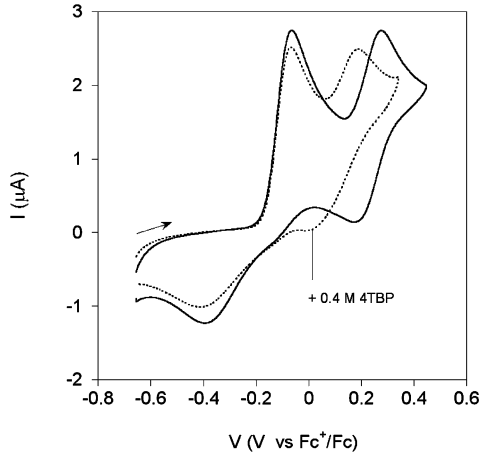

Figure 4. Cyclic voltammogram of lithium iodide in 3-methoxypropionitrile at a Pt working electrode. Electrolyte: 3 mM LiI + 0.2 M $LiClO_4$ (and 0.4 M 4TBP where indicated). The scan rate was 20 mV s^{-1}.

transport time vs light intensity is −0.61 (±0.01) for all concentrations. The 4TBP concentration has a much more pronounced effect on the electron lifetimes (τ_e) measured at open-circuit conditions. Addition of 4TBP leads to a large increase of τ_e: it increases more than 3-fold when 0 mM 4TBP and 500 mM 4TBP are compared. While the slopes of the log−log plots of τ_e vs light intensity are practically the same for 0 and 500 mM 4TBP, being −0.58 and −0.63, respectively, that for 55 mM 4TBP differs a lot (slope −0.34).

Parts b and c of Figure 3 present the measured electron lifetimes as a function of V_{OC} and Q_{OC}, respectively. An exponential decrease of τ_e with V_{OC} is clearly observed for 0 and 500 mM 4TBP, but is less clear in the case of 55 mM 4TBP. The 500 mM curve is shifted by as much as 0.35 V with respect to the 0 mM curve. Figure 3c shows the dependence of τ_e on the total electron concentration in the mesoporous TiO_2. The slopes of the log−log plots are identical for 0 and 500 mM 4TBP (−2.5), but that for 55 mM 4TBP deviates (slope −1.0). Addition of 500 mM 4TBP to the electrolyte without 4TBP led to a 17-fold increase in τ_e. The intermediate 4TBP concentration (55 mM) shows, however, a deviating response: at low Q_{OC} lifetimes are smaller and at higher Q_{OC} lifetimes larger than those found for 0 mM 4TBP.

Addition of 4TBP to the redox electrolyte has no significant effect on the measured rest potential at a Pt electrode: it was nearly constant at −0.32 ± 0.01 V vs Fc^+/Fc, corresponding to about +0.31 V vs NHE. In contrast, a significant effect of 4TBP was observed in the cyclic voltammetry (CV) of lithium iodide in 3MPN; see Figure 4. The voltammogram shows two consecutive oxidations that can be attributed to the following reactions:[29]

$$3I^- \rightleftarrows I_3^- + 2e^- \quad (1)$$

$$2I_3^- \rightleftarrows 3I_2 + 2e^- \quad (2)$$

The peaks related to reaction 2 are shifted toward negative potentials in the presence of 4TBP. This is indicative of complexation of I_2 with 4TBP.

Discussion

The potential of the TiO_2 electrode is given by the Fermi level of the electrons in the semiconductor:

$$E_F = E_C + kT \ln(n_c/N_C) \quad (3)$$

where E_F and E_C are the Fermi energy and the conduction band edge energy, respectively, kT is the thermal energy, n_c is the density of conduction band electrons, and N_C is the effective density of conduction band states. The measured potential is given by the difference between E_F in the mesoporous TiO_2 film and the redox potential of the electrolyte. No significant change in the redox potential occurred when 4TBP was added to the electrolyte. The large improvement of V_{OC}, as shown in Figure 1a, can therefore be ascribed to (1) a shift of E_C to higher energies, (2) a higher concentration of conduction band electrons under open-circuit conditions, or (3) a combined effect.

The charge extraction results shown in Figure 2a clearly demonstrate that addition of 4TBP to the electrolyte results in a shift of the electronic states in TiO_2 toward higher energies: at the same total electron concentration in the porous TiO_2 film, the voltage that is developed is higher by about 160 mV when 4TBP is present. As the increase in V_{OC} was ∼260 mV upon addition of 500 mM 4TBP, we can conclude that the additional 100 mV is caused by the presence of more conduction band electrons under open-circuit conditions.

To obtain a shift of the potential of the conduction band edge and/or trap levels of 160 mV in the negative direction, the surface charge on the microscopic area of TiO_2 needs to change by $\Delta Q_{surf} = (\Delta V)C_H \approx 1.6\ \mu C\ cm^{-2}$ or 10^{13} charges cm^{-2}, where C_H, the Helmholtz capacitance of TiO_2, is assumed to be 10^{-5} F cm^{-2}. As N719 occupies about 1.6 nm^2 per molecule,[3] they can bring at maximum 1.25×10^{14} protons cm^{-2} to the TiO_2 surface. The change in surface charge can therefore easily be accommodated by a decrease in the amount of adsorbed protons due to 4TBP that can act as a base. Alternatively, adsorbed Li^+ ions could determine the surface charge. The change in surface charge can then be explained by adsorption of 4TBP at the TiO_2 surface, thereby replacing cations.

From eq 3 it can be derived that a plot of $\ln(n_c)$ vs potential should have a slope of $(kT)^{-1} = 38.9\ V^{-1}$ at room temperature. The experimental data in Figure 2a yield, however, corresponding slopes of about 10 V^{-1}. This discrepancy was observed previously and has been explained using a trapping model.[30,31] In this model only a small fraction of the charge present in TiO_2 resides in the conduction band. Most electrons are assumed to be present in localized states (traps) below the conduction band. Several studies suggest that the density of traps in nanostructured TiO_2 increases exponentially toward the conduction band as follows:

$$N_T(E) = N_{T0} \exp\left(\frac{E - E_{F0}}{m}\right) \quad (4)$$

In this equation N_{T0} is the trap state density at E_{F0}, which is the Fermi level of TiO_2 in the dark (equal to the redox energy of the electrolyte), and m is the slope of the trap distribution. Equation 4 appears to be consistent with the data shown in Figure 2a, yielding values for m of about 100 meV. N_{T0} is about 4 times higher for 0 mM than for 55 and 500 mM 4TBP.

The above trapping model is also used to explain electron transport in nanostructured TiO_2: the transport process is then described by a multiple trapping and thermal detrapping process.[32,33] Using expressions derived by van de Lagemaat and Frank,[26] the slope of the trap distribution can be derived from transport and charge extraction measurements at short circuit. From the relation between τ_{tr} and light intensity (Figure 3a) m is calculated to be 65 meV. Similar values follow from the Q_{SC}−intensity relation (Figure 2b): m is 70, 67, and 59 meV for 0,

55, and 500 mM 4TBP, repectively. There is, however, a large discrepancy between these values and those obtained from the potential−charge relation. This poses some doubts about the validity of this trapping model.

As mentioned above, more charge is accumulated upon illumination under open-circuit conditions in the solar cell with 500 mM 4TBP in the electrolyte. This is directly related to a decrease in the recombination rate constant k_{rec} for the reaction of electrons with triiodide in the electrolyte, or in other words an increase of the electron lifetime. This was indeed measured using modulation techniques; see Figure 3. The overall recombination reaction is given by eq 5. It can be recognized that

$$I_3^- + 2e^-(TiO_2) \rightarrow 3I^- \quad (5)$$

this reaction must involve a multiple-step mechanism, where one of the steps will be rate determining. Attempts to determine the reaction order of the recombination reaction can be found in a number of papers.[8,13,34,35] Considering only the 0 and 500 mM 4TBP electrolytes, the results shown in Figure 3b,c seem to agree with a reaction that is second order in electron concentration. Figure 3b relates τ_e to V_{OC} and thereby to the concentration of conduction band electrons through eq 3: $n_C \propto \exp(V_{OC}/kT)$. A first-order reaction should therefore lead to a slope of $-38.9\ V^{-1}$ in the plot of τ_e vs V_{OC}. The experimentally found slopes of -16 and $-19\ V^{-1}$ suggest that reaction 5 is second order in the concentration of conduction band electrons. Figure 3c relates τ_e to the *total* electron concentration. The slope of -2.5 in the log−log plot suggests a reaction order of 2.5 with respect to the total electron concentration. The validity of the above approach to obtain the reaction order may, however, be questioned, as the effect of the potential energy of electrons in TiO_2 on the recombination rate is not taken into account.

If we assume that the rate-determining step of the recombination reaction is a heterogeneous electron-transfer process, the rate constant should vary exponentially with the potential of the electrons in the electrode:

$$k_{rec} = k^\circ \exp(-\alpha\eta q/kT) \quad (6)$$

where k° is the standard rate constant, α the transfer coefficient that is related to the symmetry of the energy barrier and can vary between 0 and 1, η the overpotential, which is equal to V_{OC} in our case, and q the elementary charge. If eq 6 is applied to Figure 3b, it follows that $\alpha = 0.5$. In this electrochemical approach the concentration of electrons in TiO_2 is not important, only their potential that is given by the quasi-Fermi level.

The shift of the conduction band and/or trap levels in TiO_2 upon addition of 4TBP by 160 mV in the negative direction gives a large increase of the overpotential for reduction of triiodide. One would therefore expect τ_e to decrease by a factor of ∼8 when using eq 6. Instead, τ_e increases by more than 3 orders of magnitude at equal overpotentials when 0 mM 4TBP and 500 mM 4TBP are compared (Figure 3b). This suggests that the standard rate constant for the recombination reaction k° has changed significantly due to surface modification of the TiO_2 electrode. Part of this could be caused by the more negatively charged TiO_2−electrolyte interface upon addition of 4TBP, which causes a stronger repulsion of the negatively charged triiodide ion. Another explanation could be a physical blocking of the surface or specific recombination sites on the surface by 4TBP adsorption.

The effect that 4TBP has on the electrolyte could also be of importance for the measured electron lifetimes. Cyclic voltammetry (Figure 4) shows that addition of a large concentration of 4TBP has a significant effect of the electrochemistry of iodide in 3-methoxypropionitrile. This can be attributed to binding of 4TBP with iodine. From the cyclic voltammograms in the absence of 4TBP, the formal potentials $E^{\circ\prime}$ for reactions 1 and 2 were estimated from the average of the peak potentials for oxidation and reduction ($E_1^{\circ\prime} \approx -0.24$ V, $E_2^{\circ\prime} \approx +0.21$ V vs Fc^+/Fc). As the peak split was much more than the theoretical 27 mV for a 2-electron reaction, $E^{\circ\prime}$ values should be considered as a rough estimate. The difference between $E_1^{\circ\prime}$ and $E_2^{\circ\prime}$ is directly related to the equilibrium constant K_{eq1} of equilibrium 7 between iodide and iodine.[36,37] Equation 8

$$I_2 + I^- \rightleftarrows I_3^- \quad (7)$$

$$\log K_{eq1} = \frac{2}{3}\frac{E_2^{\circ\prime} - E_1^{\circ\prime}}{0.059} \quad (8)$$

was derived from the Nernst equation for reactions 1 and 2 and the equilibrium equation of reaction 7. As $E_2^{\circ\prime} - E_1^{\circ\prime}$ was about 0.46 V, $\log K_{eq1}$ was estimated to be 5.2. A similar experiment in acetonitrile yielded a $\log K_{eq1}$ of 6.2, whereas reported values are 6.6−6.8.[36,37] Consequently, we can expect that the concentration of noncomplexed iodine is very low in 3MPN-based electrolytes, but still about 10 times higher than in acetonitrile electrolytes. In the presence of 4TBP an additional equilibrium, with equilibrium constant K_{eq2}, is expected to play a role:

$$I_2 + 4TBP \rightleftarrows I_2{-}4TBP \quad (9)$$

$E_2^{\circ\prime}$ is shifted by about 0.13 V in the negative direction upon addition of 4TBP. This can be related through the Nernst equation to a decrease in the iodine concentration by a factor of ∼27. A value for K_{eq2} of about 70 M^{-1} is calculated. This value is very small in comparison to K_{eq1} ($>10^5$ M^{-1}). Nevertheless, addition of 0.5 M 4TBP would reduce the concentration of free iodine in the 3MPN-based electrolyte from $\sim 5 \times 10^{-7}$ to $\sim 10^{-8}$ M. This could be of importance as it was shown by Durrant and co-workers that electron recombination with iodine is much faster than with triiodide.[35] In their transient absorption experiment, using acetonitrile containing 10% methanol as the solvent, they found that the recombination halftime was 2 orders of magnitude shorter with iodine than with triiodide as electron acceptor. As K_{eq1} in acetonitrile is 1 order of magnitude larger than in 3MPN, the concentration of free iodine will be about 10 times lower. This should lead to an increased electron lifetime in acetonitrile. Addition of 4TBP would only have a marginal effect on the concentration of free iodine in acetonitrile (assuming that K_{eq2} is similar in acetonitrile and 3MPN). This may explain the lack of an effect of 4TBP on the electron lifetime in the study of Nakade and co-workers, who used acetonitrile-based electrolytes.[9] It is noted, however, that such an analysis will only be valid if the reaction rate constant for iodine is much more than 2 orders of magnitude larger than that for triiodide, as the concentration of iodine is very small.

The deviating behavior of the dye-sensitized solar cells with 55 mM 4TBP in this study can tentatively be explained as follows: the lower concentration of the additive is sufficient to lead to a shift of the TiO_2 conduction band and/or trap states to more negative potentials. It will not decrease the free iodine concentration to the same extent as the higher concentration of 4TBP and gives therefore shorter electron lifetimes. Under low light intensity, at low Q_{SC}, lifetimes comparable to those observed with electrolyte lacking 4TBP were observed (Figure 3a,c). This may be caused by a competition among several

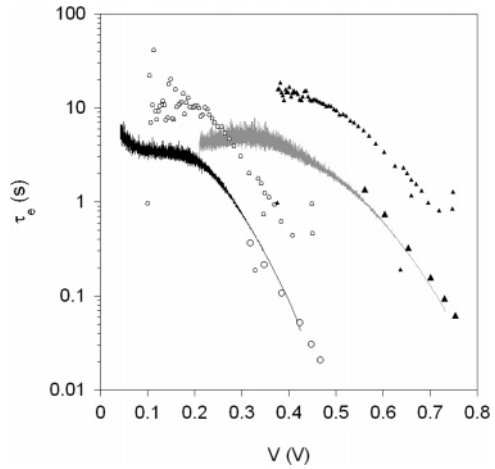

Figure 5. Comparison of electron lifetimes determined using different experimental methods: small modulation photovoltage transients (large symbols), V_{OC} decay (lines), time-dependent charge extraction (small symbols). The 4TBP concentration was either 0 mM (circles, black line) or 500 mM (triangles, gray line).

effects: the increase in τ_e due to the blocking effect of adsorbed 4TBP and due to the complexation of free iodine with 4TBP and the decrease in τ_e due to the increased overpotential for triiodide reduction.

In Figure 5, electron lifetimes determined by different experimental techniques are compared. For reasons of clarity the data of 55 mM 4TBP are not shown. The small modulation photovoltage transient technique was described above. The electron lifetime can also be calculated from the slope of a complete photovoltage decay trace (see Figure 1c) as proposed by Zaban et al..[38] Finally, τ_e can be determined from the time-dependent change of the extracted charge under open-circuit conditions, assuming first-order kinetics.[24] The observed trends in τ_e are well reproduced in all techniques: addition of 4TBP results in a large increase of the electron lifetime. While there is a good agreement between lifetimes obtained by the modulated photovoltage and V_{OC} decay methods, lifetimes obtained using the charge extraction method are much larger, by a factor of 3 (no 4TBP) to 5 (500 mM 4TBP). The reason for this discrepancy lies in the fact that the voltage methods relate electron lifetime to changes in the conduction band electron density, whereas the charge extraction method relates recombination with the total concentration of electrons in the TiO_2 film. It has been shown that the ratio between τ_e (voltage) and τ_e (charge extraction) equals kT/m for an exponential trap model (eq 4),[39] yielding $m = 77$ and 129 meV for 0 and 500 mM 4TBP, respectively. The leveling off of τ_e at low potentials is probably related to recombination occurring at the conducting glass−electrolyte interface becoming the dominant pathway.[39]

The addition of 4TBP to the electrolyte also affects the transport of electrons in the TiO_2 film. The transport time increased by ∼40% upon addition of 500 mM 4TBP, but did not change significantly upon addition of 55 mM 4TBP (Figure 3a). The effect appears even more pronounced when τ_{tr} is plotted against the total accumulated charge in TiO_2, because Q_{SC} is also increased upon 4TBP addition (see Figure S1 in the Supporting Information). The transport time in electrolyte with 500 mM 4TBP is doubled at a given Q_{SC} compared to that in electrolyte with 0 and 55 mM 4TBP. An increase in transport times has been found in acetonitrile-based electrolytes.[9] Furthermore, in conductivity studies on nanostructured TiO_2 immersed in lithium triflate electrolytes, a 30% decrease in electron mobility was found upon addition of 4TBP.[40] The origin of this effect is not clear, but it could be related to the coupled motion of electrons in TiO_2 and ions in the electrolyte that maintains charge neutrality. 4TBP might decrease the effective concentration of Li^+ ions at the TiO_2−electrolyte interface.

Conclusions

The addition of 4-*tert*-butylpyridine to the redox electrolyte of dye-sensitized TiO_2 solar cells leads to a large increase in the open-circuit potential (0.26 V in the case of 0.5 M 4TBP, 0.7 M LiI, and 0.05 M I_2 in 3-methoxypropionitrile). This can be attributed to a band edge shift of TiO_2 (responsible for 60% of the voltage increase) and to an increase of the electron lifetime (40%). 4TBP affects the surface charge of TiO_2 by decreasing the amount of adsorbed protons and/or Li^+ ions. The increase in the electron lifetime may be explained by the decreased accessibility of the TiO_2 surface for triiodide ions due to 4TBP. This argument does not seem to hold for acetonitrile-based electrolytes, where no increased lifetimes were found.[9] This could be due to the influence of the complex formation between 4TBP and iodine, which can give more pronounced effects in the case of 3-methoxypropionitrile than in the case of acetonitrile.

Optimization of the dye-sensitized solar cell is tedious work. Complex interactions between the individual components determine the final solar cell performance. By applying a combination of several experimental techniques on actual solar cells, conclusions can be drawn on the exact function of each of the components. For instance, the precise mechanisms behind the improvements that occur upon surface modification of TiO_2, either by Al^{3+} ions[41] or by organic coadsorbents such as chenodeoxycholate[42] and 4-guanidinobutyric acid,[43] were determined recently. As the secrets of the dye-sensitized solar cell are slowly unraveled, the path for optimization will become much clearer and significant improvements in the power conversion efficiency may be expected.

Acknowledgment. This work was supported by the Swedish Energy Agency and Eltra, Denmark (PSO F/U Project No. 5278).

Supporting Information Available: A plot of the relation between transport time and charge accumulated in the nanostructured TiO_2 solar cells. This material is available free of charge via the Internet at http://pubs.acs.org.

References and Notes

(1) O'Regan, B.; Grätzel, M. *Nature (London)* **1991**, *353*, 737.
(2) Nazeeruddin, M. K.; Kay, A.; Rodicio, I.; Humphry-Baker, R.; Müller, E.; Liska, P.; Vlachopoulos, N.; Grätzel, M. *J. Am. Chem. Soc.* **1993**, *115*, 6382.
(3) Hagfeldt, A.; Grätzel, M. *Acc. Chem. Res.* **2000**, *33*, 269.
(4) Nusbaumer, H.; Moser, J.-E.; Zakeeruddin, S. M.; Nazeeruddin, M. K.; Grätzel, M. *J. Phys. Chem. B* **2001**, *105*, 10461.
(5) Sapp, S. A.; Elliott, C. M.; Contado, C.; Caramori, S.; Bignozzi, C. A. *J. Am. Chem. Soc.* **2002**, *124*, 11215.
(6) Oskam, G.; Bergeron, B. V.; Meyer, G. J.; Searson, P. C. *J. Phys. Chem. B* **2001**, *105*, 6867.
(7) Wang, P.; Zakeeruddin, S. M.; Moser, J. E.; Humphry-Baker, R.; Grätzel, M. *J. Am. Chem. Soc.* **2004**, *126*, 7164.
(8) Liu, Y.; Hagfeldt, A.; Xiao, X.-R.; Lindquist, S.-E. *Sol. Energy Mater. Sol. Cells* **1998**, *55*, 267.
(9) Nakade, S.; Kanzaki, T.; Kubo, W.; Kitamura, T.; Wada, Y.; Yanagida, S. *J. Phys. Chem. B* **2005**, *109*, 3480.
(10) Kelly, C. A.; Farzad, F.; Thompson, D. W.; Stipkala, J. M.; Meyer, G. J. *Langmuir* **1999**, *15*, 7047.
(11) Tachibana, Y.; Haque, S. A.; Mercer, I. P.; Moser, J. E.; Klug, D. R.; Durrant, J. R. *J. Phys. Chem. B* **2001**, *105*, 7424.
(12) Pelet, S.; Moser, J.-E.; Grätzel, M. *J. Phys. Chem. B* **2000**, *104*, 1791.

(13) Huang, S. Y.; Schlichthörl, G.; Nozik, A. J.; Grätzel, M.; Frank, A. J. *J. Phys. Chem. B* **1997**, *101*, 2576.
(14) Schlichthörl, G.; Huang, S. Y.; Sprague, J.; Frank, A. J. *J. Phys. Chem. B* **1997**, *101*, 8139.
(15) Boschloo, G.; Lindström, H.; Magnusson, E.; Holmberg, A.; Hagfeldt, A. *J. Photochem. Photobiol., A* **2002**, *148*, 11.
(16) Kusama, H.; Konishi, Y.; Sugihara, H.; Arakawa, H. *Sol. Energy Mater. Sol. Cells* **2003**, *80*, 167.
(17) Shi, C.; Dai, S.; Wang, K.; Pana, X.; Kong, F.; Hu, L. *Vib. Spectrosc.* **2005**, *39*, 99−105.
(18) Reid, C.; Mulliken, R. S. *J. Am. Chem. Soc.* **1954**, *76*, 3869.
(19) Tassaing, T.; Besnard, M. *J. Phys. Chem. A* **1997**, *101*, 2803.
(20) Kebede, Z.; Lindquist, S.-E. *Sol. Energy Mater. Sol. Cells* **1999**, *57*, 259.
(21) Greijer, H.; Lindgren, J.; Hagfeldt, A. *J. Phys. Chem. B* **2001**, *105*, 6314.
(22) Lindström, H.; Magnusson, E.; Holmberg, A.; Södergren, S.; Lindquist, S.-E.; Hagfeldt, A. *Sol. Energy Mater. Sol. Cells* **2002**, *73*, 91.
(23) Duffy, N. W.; Peter, L. M.; Rajapakse, R. M. G.; Wijayantha, K. G. U. *Electrochem. Commun.* **2000**, *2*, 658.
(24) Boschloo, G.; Hagfeldt, A. *J. Phys. Chem. B* **2005**, *109*, 12093.
(25) Kopidakis, N.; Benkstein, K. D.; van de Lagemaat, J.; Frank, A. J. *J. Phys. Chem. B* **2003**, *107*, 11307.
(26) van de Lagemaat, J.; Frank, A. J. *J. Phys. Chem. B* **2000**, *104*, 4292.
(27) Duffy, N. W.; Peter, L. M.; Wijayantha, K. G. U. *Electrochem. Commun.* **2000**, *2*, 262−266.
(28) O'Regan, B.; Lenzmann, F. *J. Phys. Chem. B* **2004**, *108*, 4342.
(29) Popov, A. I.; Geske, D. H. *J. Am. Chem. Soc.* **1958**, *80*, 1340.
(30) Peter, L.; Duffy, N.; Wang, R.; Wijayantha, K. *J. Electroanal. Chem.* **2002**, *524*, 127.
(31) Fabregat-Santiago, F.; Mora-Sero, I.; Garcia-Belmonte, G.; Bisquert, J. *J. Phys. Chem. B* **2003**, 758.
(32) de Jongh, P. E.; Vanmaekelbergh, D. *Phys. Rev. Lett.* **1996**, *77*, 3427.
(33) Dloczik, L.; Ileperuma, O.; Lauermann, I.; Peter, L.; Ponomarev, E.; Redmond, G.; Shaw, N.; Uhlendorf, I. *J. Phys. Chem. B* **1997**, *101*, 10281.
(34) Fisher, A. C.; Peter, L. M.; Ponomarev, E. A.; Walker, A. B.; Wijayantha, K. G. U. *J. Phys. Chem. B* **2000**, *104*, 949.
(35) Green, A. N. M.; Chandler, R. E.; Haque, S. A.; Nelson, J.; Durrant, J. R. *J. Phys. Chem. B* **2005**, *109*, 142.
(36) Nelson, I. V.; Iwamoto, R. T. *J. Electroanal. Chem.* **1964**, *7*, 218.
(37) Datta, J.; Bhattacharya, A.; Kundu, K. K. *Bull. Chem. Soc. Jpn.* **1988**, *61*, 1735.
(38) Zaban, A.; Greenshtein, M.; Bisquert, J. *ChemPhysChem* **2003**, *4*, 859.
(39) Cameron, P. J.; Peter, L. M. *J. Phys. Chem. B* **2005**, *109*, 7392.
(40) Greijer-Agrell, H.; Boschloo, G.; Hagfeldt, A. *J. Phys. Chem. B* **2004**, *108*, 12388.
(41) Alarcon, H.; Boschloo, G.; Mendoza, P.; Solis, J. L.; Hagfeldt, A. *J. Phys. Chem. B* **2005**, 18483.
(42) Neale, N. R.; Kopidakis, N.; van de Lagemaat, J.; Grätzel, M.; Frank, A. J. *J. Phys. Chem. B* **2005**, *109*, 23183.
(43) Zhang, Z.; Zakeeruddin, S. M.; O'Regan, B. C.; Humphry-Baker, R.; Grätzel, M. *J. Phys. Chem. B* **2005**, *109*, 21818.